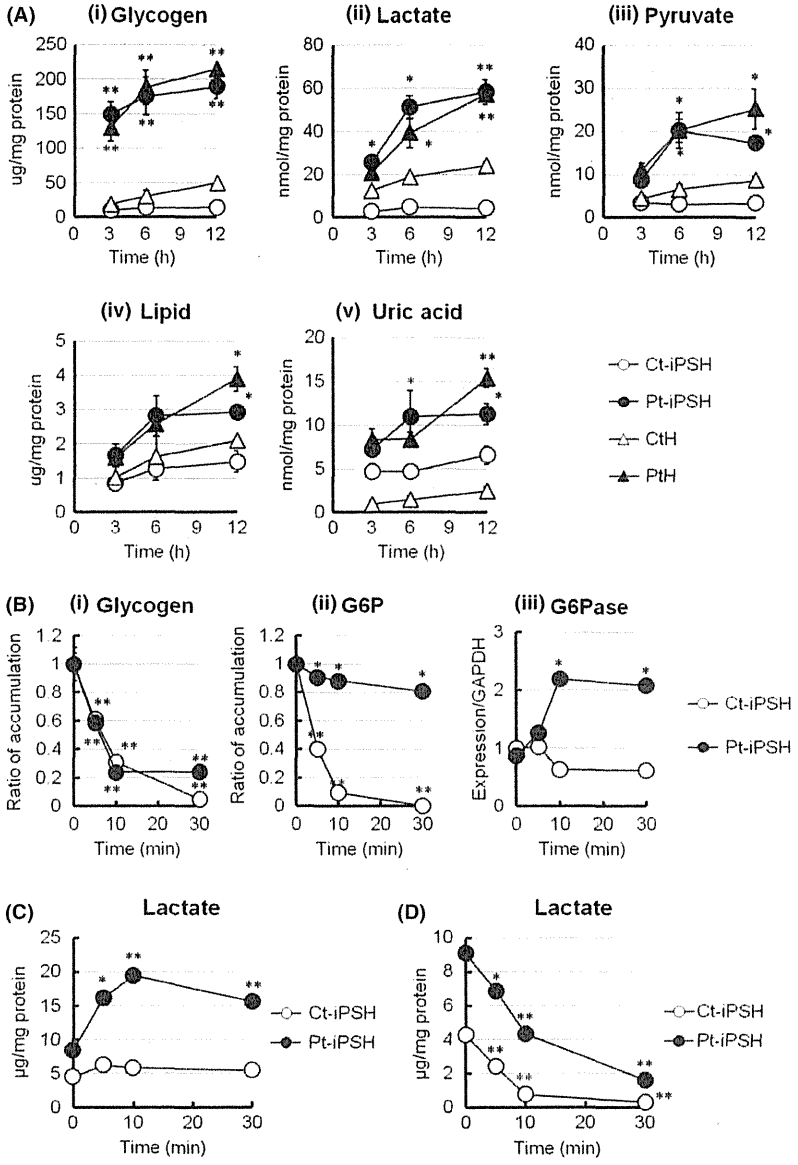

Figure 4 Analyses of metabolic functions of glycogen storage disease type Ib-induced pluripotent stem cells (GSDIb-iPSCs)-derived hepatocytes. (A) GSDIb-iPSC-derived hepatocytes secreted more glycogen (i), lactate (ii), pyruvate (iii), lipid (iv) and uric acid (v) than those of the control subjects as assessed by quantitative determinations at 3, 6 and 12 h. *, **$P < 0.05$, 0.01 versus control-iPSC-derived hepatocytes (Ct-iPSH). (B) Glucagon administration assay. Glycogen accumulation, glucose-6-phosphate (G6P) accumulation and glucose-6-phosphatase (G6Pase) gene expression levels were calculated as the ratio to the value for each iPS-derived hepatocyte level at 0 min. Galactose (C) and glucose (D) administration assay. *, **$P < 0.05$, 0.01 versus each iPSH at 0 min (B–D). Pt-iPSH, GSDIb-iPSC-derived hepatocytes; PtH, GSDIb patient's hepatocytes; CtH, normal hepatocytes. Data are expressed as the mean ± standard error of three independent experiments.

Information). Among these, the mesodermal markers *FLK1*, *BRACHYURY* and *RUNX1* were expressed after 14 days of differentiation. Neutrophil markers *PU.I*, Myeloperoxidase (*MPO*), lactoferrin (*LTF*), gelatinase (*MMP9*), GATA-binding protein 2 (*GATA2*) and CCAAT-/enhancer-binding protein epsilon (*CEBPe*) appeared on day 23, and these markers were up-regulated until day 32.

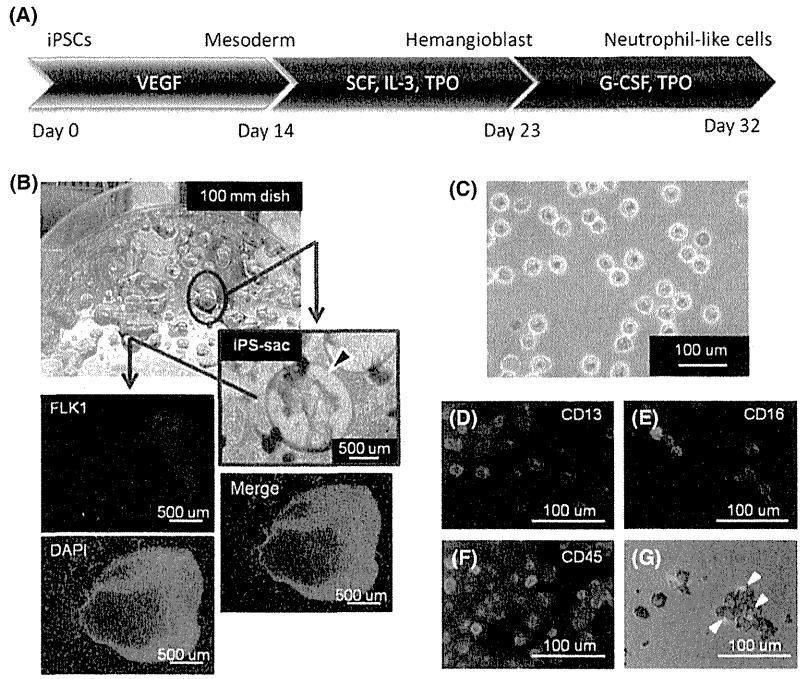

Figure 5 Differentiation of glycogen storage disease type Ib-induced pluripotent stem cells (GSDIb-iPSCs) into neutrophils. (A) Flow chart showing the differentiation protocol. VEGF, vascular endothelial growth factor; SCF, stem cell factor; IL-3, interleukin-3; TPO, thrombopoietin; G-CSF, granulocyte colony-stimulating factor. (B) iPS-sac(s) (day 23, arrow). FLK1 was highly expressed on the surface of iPS-sacs. (C) GSDIb-iPSC-derived neutrophil-like cells (day 32). Immunofluorescent staining of CD13 (D), CD16 (E) and CD45 (F). (G) Zymosan uptake assay of phagocytic capacity.

On day 32, cells were suspended in culture medium and then collected and subjected to immunostaining. As shown in Fig. 5D–F, these cells were positive for CD13, CD16 and CD45. Moreover, when differentiated cells were incubated at 37 °C for 30 min in the presence of zymosan A, phagocytosis of fluorescently labeled zymosan A was observed (Fig. 5G).

Figure 6A shows the assessment of oxidative stress using dihydroethidium staining. Reduced ethidium readily permeates cell membranes and gives an orange color when oxidized inside cells. Ethidium appeared brighter in neutrophils from GSDIb-iPSCs compared with the control iPSCs. In addition, chemiluminescence resulting from the reaction of oxygen metabolites inside cells (O_2^- and $HClO^-$) with 8-amino-5-chloro-7-phenylpyridol [3,4-d]pyridazine-1, 4-(2H,3H)dione sodium salt (L-012) was also greater in iPSCs from patients with GSDIb (Fig. 6B). The same results were obtained for all Pt-iPSC lines studied here, and the vitamin E (VE)-derivative tolorox C reduced oxidative stresses in these cells as well.

Figure 7A shows the exposure of phosphatidylserine on the surface of cell membranes, as shown using fluorescent FITC-labeled annexin V that has high and specific affinity for phosphatidylserine. As shown in Fig. 7A, neutrophils that had differentiated from GSDIb-iPSCs had greater FITC fluorescence than control cells. Caspases are a family of cysteine proteases that are involved in signaling pathways that trigger apoptosis (Li *et al.* 1997; Scott *et al.* 2005). Similar to annexin V, caspase-3 and caspase-9 in neutrophils from GSDIb-iPSCs were approximately two- to fivefold more active, respectively, than those in controls (control iPSCs and control neutrophils; Fig. 7B,C). In the present study, the VE-derivative tolorox C reduced oxidative stress and the activity of caspase-3 and caspase-9, which are markers of apoptosis.

Discussion

The use of iPSCs need not be limited to regenerative medicine. By producing iPSCs from the patient's cells

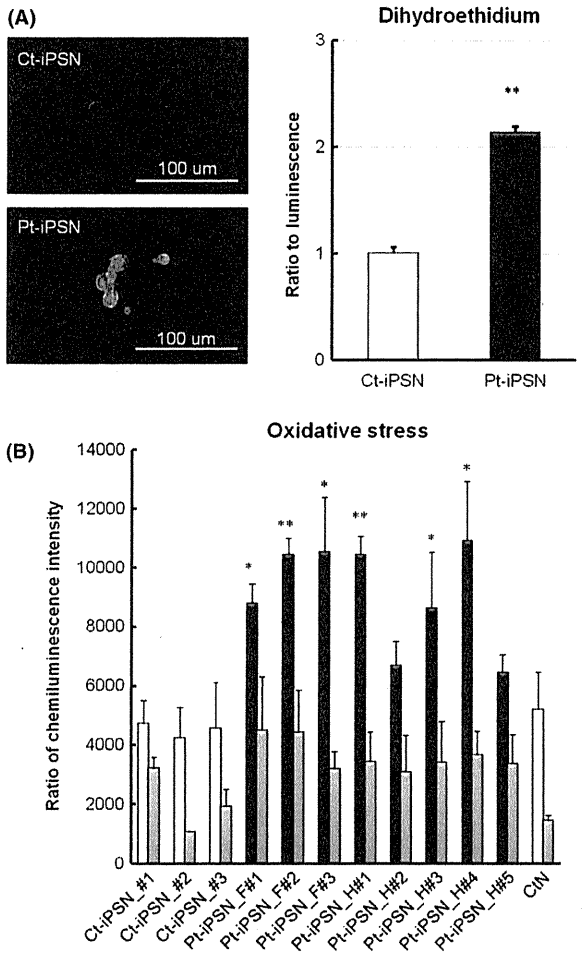

Figure 6 Glycogen storage disease type Ib-induced pluripotent stem cell (GSDIb-iPSC)-derived neutrophils exhibit increased oxidative stress. GSDIb-iPSCs were differentiated into neutrophils and assessed for their characteristics that reflect GSDIb pathology. (A) Neutrophils differentiated from iPSCs were stained with dihydroethidium. The fluorescence intensity of GSDIb-iPSC-derived neutrophil-like cells (Pt-iPSNs) was greater than that of control-iPSC-derived neutrophil-like cells (Ct-iPSNs). Expression levels calculated as the ratio to the value of the Ct-iPSN. $^{**}P < 0.01$ versus Ct-iPSNs. (B) Analysis of oxidative stress. Cells were pre-incubated with the superoxide-sensitive chemiluminescent dye L-012. The rate of superoxide anion generation was measured using a luminometer. Each gray column represents the results of cells treated with vitamin E. Data are expressed as the mean ± standard error of four independent experiments. *, $^{**}P < 0.05$, 0.01 versus normal neutrophils (CtN).

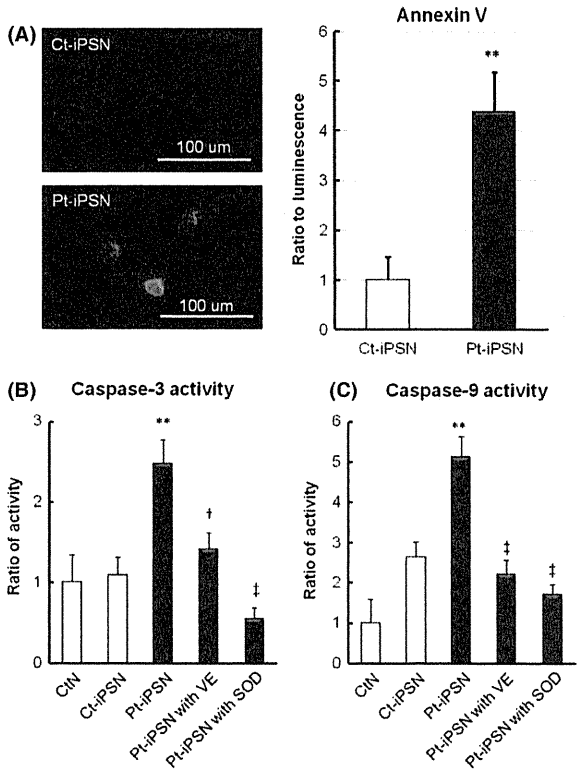

Figure 7 Glycogen storage disease type Ib-induced pluripotent stem cells (GSDIb-iPSCs)-derived neutrophils display increased apoptosis. (A) Annexin V-positive neutrophils, as determined by fluorescence staining (green; FITC). The fluorescence of the GSDIb-iPSC-derived neutrophil-like cells (Pt-iPSNs) was more intense than that of the control-iPSC-derived neutrophil-like cells (Ct-iPSN). Expression levels were calculated as the ratio to that of the respective Ct-iPSN. $^{**}P < 0.01$ versus Ct-iPSN. (B,C) Analysis of caspase activity. The DEVD-cleaving activity of caspase-3 (B) and the LEHD-cleaving activity of active caspase-9 (C) in protein extracts of differentiated cells. Expression levels were calculated as the ratio to that of the value of the respective control neutrophils (CtN). Data are expressed as the mean ± standard error of three independent experiments. *, $^{**}P < 0.05$, 0.01 versus CtNs; †, ‡$P < 0.05$, 0.01 versus Pt-iPSN. VE, vitamin E; SOD, superoxide dismutase.

and inducing differentiation into specific cell types, this technology can provide cell types that are otherwise difficult to collect. Thus, iPSCs can facilitate research into the causes and mechanisms of diseases that had previously gone untreated (Lee *et al.* 2009; Ye *et al.* 2009). In this study, we established iPSCs from patients with GSDIb and replicated the phenotype.

Gene expression analysis showed that the expression of genes during the differentiation process of GSDIb-iPSCs recapitulated that of the liver developmental stage (Fig. 2 and Fig. S4 in Supporting

Information). The first step involved driving differentiation of human iPSCs to endodermal cells that expressed *SOX17* and *GSC*. In contrast, *OCT4* and *NANOG* were down-regulated in GSDIb-iPSCs. The resulting endodermal cells were then differentiated into hepatic progenitors that express *HNF4α*. The early fetal hepatic marker *AFP*, which also represents endodermal differentiation, has decreased expression as the liver develops (Chou 1988). In these experiments, *AFP* was expressed by day 12 and was maintained until day 20. In contrast, *ALB* mRNA appeared at approximately day 20 and increased with the duration of the differentiation period. We observed ALB-positive cells at day 25 as well as *ALB* mRNA expression (Fig. 2G). Importantly, neither *ALB* nor *AFP* mRNA was almost detectable in undifferentiated iPSCs. The expression of *TAT*, *CYP7A1*, *G6Pase*, *PFK1*, *PGMase*, *CYP1A2*, *CYP2D6*, *CYP3A4*, *CYP3A5* and *CYP3A7* mRNA was also detectable on day 25 (Fig. S5 in Supporting Information). The cells showed characteristic hepatocyte morphologies, including a polygonal shape and distinct round nuclei. These results indicate that this protocol for differentiation of human iPSCs into hepatocytes successfully imitated the natural developmental processes of hepatocytes.

Uptake and release of compounds from the circulation is an important hepatocyte function (Muller & Jansen 1998). For example, the nontoxic organic anion ICG is eliminated exclusively by mature hepatocytes and is used clinically to test hepatic function (Berk & Stremmel 1986). In this study, we used uptake and release of ICG to identify hepatocytes derived from iPSCs (Fig. 2H), as previously achieved with ESCs (Yamada *et al.* 2002). Differentiated cells displayed a pronounced capacity to take up ICG (Fig. 2H upper) and release it 6 h later (Fig. 2H lower). These results suggest that iPSC-derived hepatocytes are functional and bear characteristics of liver hepatocytes.

The inborn error of metabolism GSDIb is caused by a genetic defect in the G6P transporter found on endoplasmic reticulum membranes (Narisawa *et al.* 1978). This in turn results in hypoglycemia because glucose in the liver cannot be released into the circulation. Glycolysis is also overly induced in these cells, increasing glycogen storage and causing hyperlactacidemia and hyperlipidemia. These symptoms are the same as those of GSDIa, which is caused by G6Pase gene mutations (Melis *et al.* 2007). Hepatocytes differentiated from GSDIb-iPSCs in the current study were found to have classic symptoms of GSDI, including excessive glycogen storage. Experiments using PAS staining showed excessive accumulation of intracellular glycogen in GSDIb-iPSCs-derived hepatocytes compared with iPSC-derived hepatocytes from control subjects (Fig. 3A), and also, a lipid-specific staining showed excessive accumulation of intracellular lipid (Fig. 3B). This finding agrees with that of Rashid *et al.* (2010), who reported an iPSC model of GSDIa. In addition, we analyzed other iPSC lines. As shown in Fig. 3D, increased accumulation of glycogen was detected in iPSH derived from patient with GSDIb compared with iPSH from the control group. Moreover, metabolic analyses showed typical symptoms of GSDIb, including glycogen accumulation, hyperlactacidemia and hyperlipidemia (Fig. 4A).

Glucagon activates adenylate cyclase in the liver producing cyclic AMP, which activates the phosphorylase system to promote glycogen digestion and increase the concentration of blood sugar. Because the phosphorylase system of patients with GSDIb is normal, generation of glucose-1 phosphate from glycogen and its conversion to G6P progress normally. However, the converted G6P flows into the G6Pase system to maintain blood sugar level, and glycolysis is required for energy utilization. In patients with GSDIb, the G6Pase system is impaired, and G6P production induced by glucagon is consumed by glycolysis. In the present study, G6P metabolism was delayed in hepatocytes derived from patients with GSDIb, and the levels of glycolytic enzymes were continuously increased compared with controls. The clinical classification screening method reported by Fernandes *et al.* (1974) allowed us to detect short-term decreases in the level of lactic acid caused by glucose administration (Fig. 4D). Furthermore, lactate storage was increased in GSDIb-iPSCs by galactose administration (Fig. 4C). These results suggest that iPSC-derived hepatocyte-like cells express the phenotype of patients with GSDIb.

The gene expression patterns of pluripotency markers, transcription factors and granule proteins during neutrophil differentiation in this culture system were investigated using qPCR (Fig. S5 in Supporting Information). We observed mesodermal cell markers, such as *FLK1*, *BRACHYURY* and *RUNX1*, which confirmed differentiation into mesodermal cells at day 14 (Fig. S5A in Supporting Information). Immediately after culturing from days 14 to 23, domed structures (iPS-*sacs*) were observed (Fig. 5B). The *sacs* are generally said to reflect the secondary hematopoietic mechanism. The *sacs* exist as vascular endothelial-like cells, and hemocytes with the same

origin as the endothelial-like cells are induced inside the *sacs*. In the present study, we confirmed that the surface of the *sacs* was FLK1-positive (Fig. 5B; endothelial-like cells). When their *sacs* were burst, numerous spherical cells were observed inside (days 23–32). On day 23, essential transcription factors for commitment and differentiation of the granulocytic lineage, including *PU.I* (Borregaard *et al.* 2001; Friedman 2007), appeared (Fig. S5B in Supporting Information). On this day, *LTF* and *MPO*, which are highly expressed in myeloblasts and promyelocytes, and myelocytes and metamyelocytes, respectively (Cowland & Borregaard 1999; Borregaard *et al.* 2001), were also detected. *MMP9*, *GATA2* and *CEBPe*, which are highly expressed in band and segmented neutrophilic cells (Cowland & Borregaard 1999; Borregaard *et al.* 2001), were also detected. Gene expression analyses showed that the differentiation process of GSDIb-iPSCs recapitulated that of normal neutrophil development. Collectively, these results suggested that neutrophil differentiation in this coculture system may recapitulate the orderly differentiation process of bone marrow.

On day 32, CD13-, CD16- and CD45-positive cells were observed (Fig. 5D–F). The CD13 antigen is found on the vast majority of myeloid cells such as neutrophils, eosinophils, basophils and monocytes of normal peripheral blood. These antigens are found on the surface of precursors to myeloid differentiation (Sakai *et al.* 1987). Similarly, CD16 (glycosyl phosphatidylinositol-linked) is expressed in neutrophils (Lanier *et al.* 1989), and CD45 is expressed on the surface of all human leukocytes, but is not present in erythrocytes and platelets (Pulido *et al.* 1989). Because the cells on day 32 were positive for all three markers, differentiation of iPSCs into neutrophils was confirmed.

Leukocytes eliminate invading microbes, remove damaged cells and foreign matter and play a key role in defense against infection (Fasske & Morgenroth 1985). Zymosan is a component of the yeast cell wall that is phagocytosed by leukocytes despite being opsonized (Czop 1986). When iPSC-derived neutrophils were incubated in the presence of fluorescently labeled zymosan A, phagocytosis was observed (Fig. 5G), indicating that iPSCs had differentiated into functional neutrophils.

The characteristic symptoms of GSDIb differ from those of GSDIa. Whereas the former is characterized by neutrophil dysfunction or neutropenia and carries a greater risk of frequent infection (Kuijpers *et al.* 2003), G6Pase-α, the gene responsible for GSDIa, is not expressed in neutrophils (Guionie *et al.* 2003). iPSCs in the current study originated from patients with GSDIb. These patients had a neutrophil count below 1000/μL that was maintained with a G-CSF preparation, and infection was being prevented with antibiotics (Donadieu *et al.* 2011; Visser *et al.* 2012). Whether neutrophil G6PT is associated with neutropenia or neutrophil dysfunction has not been clarified, although it induces oxidative stress and promotes apoptosis (Melis *et al.* 2008). Using a mouse model of GSDIb, Kim *et al.* (2008) reported that oxidative stress continued to increase in mouse neutrophils and led to increased activity of caspase-3 and caspase-9. In GSDIb, neutropenia follows disruption of the G6Pase system. This was shown by Cheung *et al.* (2007) who found neutrophil-specific G6Pase-β in G6Pase-β-knockout mice. An increase in oxidative stress and development of apoptosis were noted in the model of patient cells established in the current study, and the phenotype of the patient's condition was indicated. Antioxidants reverse neutropenia in patients with GSDIb after administration of antioxidants (Melis *et al.* 2008). It is believed that antioxidant administration is effective because of the improvement in apoptosis of neutrophils. In the present study, the VE-derivative tolorox C reduced oxidative stress and the activity of markers of apoptosis, caspase-3 and caspase-9 (Fig. 7B,C). These results are the first to show the effectiveness of antioxidants on clinical sites in a human *in vitro* model. Whereas the current study was unable to clarify the mechanisms of the condition, future studies using this cell model will characterize the condition and its treatments.

Experimental procedures

Materials

Human control iPSC lines, obtained from Umezawa *et al.* National Center for Child Health and Development, were used as control iPSCs. The OP9 cells and myeloid cells were obtained from Riken BRC (Tokyo, Japan). MEF were purchased from Oriental Yeast (Tokyo, Japan). Dulbecco's modified Eagle's medium (DMEM), DMEM and Ham's nutrient mixture F-12 (DMEM/F12), MEMα, oncostatin M, dexamethasone, L-012, dihydroethidium and DAPI solution were from Wako Pure Chemicals (Osaka, Japan). Fetal bovine serum (FBS), polyethylenimine, ICG, the leukocyte alkaline phosphatase kit and the PAS kit were from Sigma-Aldrich (St. Louis, MO, USA). SYBR Premix ExTaqII was from Takara Bio (Osaka, Japan). The Platinum ES/EC Retrovirus Expression System (Pantropic) was from Cell Biolabs, Inc. (San Diego, CA, USA). Knockout serum replacement (KSR),

knockout DMEM (KO-DMEM), RPMI + GlutaMax, GlutaMax, collagenase IV, superscript II reverse transcriptase, Alexa Fluor 488 (goat anti-mouse IgM and rabbit IgG), Alexa Fluor 568 (goat anti-mouse IgG and rabbit IgG), Alexa Fluor 488-conjugated zymosan A and boron dipyrromethene were from Invitrogen Life Science (Carlsbad, CA, USA). Basic fibroblast growth factor (bFGF), activin A, hepatocyte growth factor, VEGF, IL-3, SCF, TPO and G-CSF were from Pepro Tech (Rocky Hill, NJ, USA). Cosmedium 004 was from Cosmo Bio (Tokyo, Japan). Polybrene was from Nacalai Tesque (Kyoto, Japan), and the RNeasy Mini Kit was from Qiagen (Valencia, CA, USA). Glycogen, D-lactate, pyruvate, adipogenesis and ureic acid assay kits, ES/iPS cell characterization kit, anti-human SOX17 and anti-human TUJ1 were from Funakoshi (Tokyo, Japan). Anti-human albumin (ALB) antibody and anti-human FLK1 were from Abcam (Cambridge, UK). Anti-human CD13, CD16 and CD45, and BD Matrigel Matrix (growth factor reduced) were from BD Biosciences (Bedford, MA, USA). Annexin V-FITC was from Medical Biological Laboratories (Nagoya, Japan). The Bio-Rad protein assay kit was from Bio-Rad Laboratories (Hercules, CA, USA). Human liver cells were purchased from DS Pharma Biomedical (Osaka, Japan). All other reagents were of the highest quality available.

Subjects

The GSDIb patient of this study was 2 years of age and was diagnosed with GSDIb after genetic screening. We used resected tissues from the living donor liver transplantation. Protocols for research involving human subjects were approved by the institutional ethical committee of the Nagoya City University, Graduate School of Medical Sciences, Nagoya, Japan, and the National Center for Child Health and Development, Tokyo, Japan. All the study participants provided written informed consent.

Cell culture

After getting the appropriate ethical approval and patient consent, dermal fibroblasts and hepatic nonparenchymal cells were derived from donated tissue and were grown in standard fibroblast culture medium: DMEM containing 10% FBS and 0.5% penicillin and streptomycin.

Retroviral infection and generation of iPSCs

The five classic retroviral vectors pMXs-hOCT4, pMXs-hSOX2, pMXs-hKLF4, pMXs-hNANOG and pMXs-hGLIS1 encoding reprogramming factors from the laboratory of Dr. Yamanaka were obtained from Addgene (Cambridge, MA, USA). Retroviral supernatants were produced by transfection of Plat-GP cells in polyethylenimine transfection reagent using a mixture of two plasmids: a transducing vector and a plasmid expressing the VSV-G envelope protein gene.

Dermal fibroblasts and liver hepatic nonparenchymal cells were seeded at 2×10^5 cells per 60-mm dish 1 day before transduction. The medium was replaced with virus-containing supernatant supplemented with 4 μg/mL polybrene and was incubated for 24 h. Seven days after introduction, the cells were harvested by trypsinization and plated onto mitomycin C-treated MEF at 6×10^5 cells per 100-mm dish. At the same time, DMEM containing 10% FBS was replaced with medium for iPSC culture that consisted of DMEM/F12 supplemented with 20% KSR, 2 mM L-glutamine, 0.2 mM nonessential amino acids (NEAA), 0.1 mM β-mercaptoethanol and 5 ng/mL bFGF. The medium was exchanged every other day. Three to 5 weeks after induction, colonies were picked and dissociated mechanically into small clumps by pipetting up and down. The cell suspension was transferred onto MEF in 60-mm dish and cultured in 2 mL of medium for iPSC culture. For cell splitting, undifferentiated iPSC colonies were detached from the feeder cells using 0.25% trypsin supplemented with 0.1% collagenase IV, 1 mM $CaCl_2$ and 20% KSR. The removed colonies were dissociated mechanically and replated on a new mitomycin C-treated MEF feeder layer.

EB formation

The iPSC colonies were used to form EBs. After replacement with EB medium (KO-DMEM containing 20% FBS, 2 mM L-glutamine, 2 mM NEAA and 0.1 mM β-mercaptoethanol), the iPSC colonies were scraped in parallel along the periphery three times without enzymes. The scraped colonies were transferred into 100-mm plates (As one, Tokyo, Japan) without pipetting and were cultured for 7 days. The medium was exchanged on days 3–4.

In vitro differentiation, differentiation of patient with iPSCs treated with activin A

To induce differentiation, we cultured patient iPSCs using the modified Okabayashi and Asashima method (Okabayashi & Asashima 2003). The iPSCs were cultured in RPMI medium containing 0.5% FBS and GlutaMax supplemented with 0.5, 10 or 100 ng/mL activin A to drive differentiation of human iPSCs into triploblastic cells. On the third day, the medium was changed to RPMI containing 2% KSR and GlutaMax supplemented with 0.5, 10 or 100-ng/mL activin A. The cells were then cultured for 5 days.

Differentiation of human iPSCs to hepatocytes

The iPSCs were cultured in RPMI medium containing 0.5% FBS and GlutaMax supplemented with 100 ng/mL activin A to drive differentiation of human iPSCs into definitive endoderm. On the third day, the medium was changed to RPMI containing 2% KSR and GlutaMax supplemented with 100 ng/mL activin A. To differentiate human iPSCs into hepatoblast, activin A-treated cells were then cultured for

5 days in KO-DMEM containing 1% DMSO, GlutaMax, NEAA and 20% KSR. Finally, to mature the resulting hepatic hepatoblast, cells were cultured in Cosmedium 004 supplemented with 10 ng/mL hepatocyte growth factor, 20 ng/mL oncostatin M and 100 nM dexamethasone.

Differentiation of human iPSCs to neutrophils

Human iPSCs were differentiated into neutrophils according to the method of Morishima *et al.* (2011). The iPSCs were seeded onto the OP9 cells and were cultured in MEMα medium containing 10% FBS medium supplemented with 20 ng/mL VEGF to drive differentiation of human iPSCs into definitive mesoderm. After 9 days, induced cells were seeded onto fresh OP9 cells and were cultured in MEMα containing 10% FBS supplemented with 20 ng/mL IL-3, 50 ng/mL SCF and 10 ng/mL TPO for 9 days. Finally, to induce differentiation into neutrophils, cytokines were changed to 20 ng/mL IL-3 and 10 ng/mL G-CSF and cultured for 9 days.

RNA extraction and PCR

Total RNAs were extracted from human iPSCs or differentiated progenitors using the RNeasy Mini Kit (Qiagen). For each sample, 0.5 μg of total RNA was reverse-transcribed using superscript II reverse transcriptase. Real-time PCR mixtures were prepared according to the SYBR Green protocol, then denatured at 95 °C for 30 s, cycled 30 times at 95 °C for 5 s and 60 °C for 31 s, followed by a final extension at 72 °C for 10 min. Real-time PCRs were carried out using a 7300 Real-Time PCR System (Applied Biosystems). The RT-PCR was carried out using a 2720 Thermal Cycler (Applied Biosystems). Amplified products were separated by electrophoresis on a 2% agarose gel and stained with ethidium bromide. Primers used for PCR analyses are shown in Table 1.

AP staining

Alkaline phosphatase staining was carried out on cells using a leukocyte alkaline phosphatase kit according to the manufacturer's instructions. Cells were washed out with PBS and fixed to slides by immersing in citrate-buffered acetone for 30 s, rinsed gently in MilliQ water for 45 s, and then incubated with alkaline–dye mixture for 30 min. After 30 min, the slides were removed and rinsed thoroughly in MilliQ water for 2 min.

Immunostaining

Cells were fixed for 20 min at 4 °C in 4% paraformaldehyde and then washed three times in PBS. Cells were incubated for 20 min at room temperature in PBS containing 10% bovine serum and subsequently incubated overnight at 4 °C with the following primary antibodies, diluted in PBS: Oct-3/4 (1 : 100), NANOG (1 : 100), TRA-1-60 (1 : 100), SSEA3 (1 : 100), TUJ1 (1 : 200), FLK1 (1 : 200), SOX17 (1 : 200) and ALB (1 : 200). Cells were then washed three times in PBS and incubated with Alexa Fluor 488 or 568-conjugated anti-mouse IgG (1 : 200) or IgM (1 : 200) or rabbit IgG (1 : 200) for 1 h at room temperature. Unbound secondary antibody was removed by three washes in PBS. The iPSC-derived neutrophils were fixed with methanol and stained with R-phycoerythrin (PE)-conjugated antibodies for CD13, CD16 and CD45 for 10 min. After staining, cells were washed with running MilliQ water for 5 min. Simultaneous excitation at 488 and 585 nm was used to visualize the green fluorescence of PE. For lipid visualization, a lipid-specific stain boron dipyrromethene was used.

Cellular uptake and release of ICG

A 5 mg/mL stock solution of ICG was prepared in MilliQ water and was freshly diluted in culture medium to 1 mg/mL. Cells were incubated in diluted ICG for 60 min at 37 °C and then rinsed three times with PBS. Culture dishes were refilled with Cosmedium 004 and incubated for another 6 h. Cellular uptake and release of ICG were examined by microscopy.

PAS staining

Differentiated human iPSCs were fixed in 4% paraformaldehyde for 60 min and were then treated with 1% periodic acid solution for 5 min. After rinsing three times in PBS, cells were exposed to Schiff's reagent for 15 min at room temperature and then washed under running MilliQ water for 5 min. After 5 min, the cells were dehydrated with ethanol and examined using a Nikon ECLIPSE Ti microscope with a Nikon digital camera DS-U3.

Measurement of glycolytic products

After differentiation of human iPSCs into hepatocyte-like cells, the medium was replaced with Cosmedium 004, and cells were harvested after 3, 6 or 12 h. Measurement of glycolysis products such as glycogen, lactate, pyruvate and lipid were carried out on cells in triplicate using glycogen, D-lactate, pyruvate, adipogenesis and ureic acid assay kits, respectively.

In the glucagon administration assay, the medium was replaced with Cosmedium 004, iPS-derived hepatocytes were cultured for 12 h, the medium was changed to a DMEM glucose-free medium (100 nM glucagon, 2 mM L-glutamine and 0.5% BSA), and the culture fluid was sampled at the indicated time intervals. Quantitation of glycogen and G6P levels was carried out using a G6P assay kit according to the manufacturer's instructions.

In the glucose administration assay, iPS-derived hepatocytes were cultured for 30 min in DMEM glucose-free medium containing 2 mM L-glutamine and 0.5% BSA. After 30 min, glucose was added to a final concentration of 10 mM. The

Table 1 Sequences of primers for PCR analysis

Primer name	Forward primer sequence (5′ to 3′)	Reverse primer sequence (5′ to 3′)
ALB	GAGCTTTTTGAGCAGCTTGG	GGTTCAGGACCACGGATAGA
AFP	AGCTTGGTGGTGGATGAAAC	TCTGCAATGACAGCCTCAAG
BRACHYURY	ACCCAGTTCATAGCGGTGAC	CAATTGTCATGGGATTGCAG
CEBPe	CCCTTACACAAGGGCAAGAA	CTCTGCCATGTACTCCAGCA
CYP1A2	CCTCTTTGGAGCTGGGTTTG	GCTGTGGGGGATGGTGAA
CYP2D6	CCTACGCTTCCAAAAGGCTTTT	AGAGAACAGGTCAGCCACCACT
CYP3A4	CTGTGTGTTTCCAAGAGAAGTTAC	TGCATCAATTTCCTCCTGCAG
CYP3A5	CTCTCTGTTTCCAAAAGATACC	TGAAGATTATTGACTGGGCTG
CYP3A7	AGATTTAATCCATTAGATCCATTCG	AGGCGACCTTCTTTTATCTG
CYP7A1	TAGGAACCCAGAAGCAATGA	GGATGTTGAGGGAGGCACTGG
FLK1	CTGCAAATTTGGAAACCTGTC	GAGCTCTGGCTACTGGTGATG
G6Pase	TTTGGGATCCAGTCAACACA	CAGATGGGGAAGAGGACGTA
GAPDH	GAGTCAACGGATTTGGTCGT	GACAAGCTTCCCGTTCTCAG
GATA2	ACCGGAAGATGTCCAACAAG	TCTCCTGCATGCACTTTGAC
GDF3	AAATGTTTGTGTTGCGGTCA	TCTGGCACAGGTGTCTTCAG
GSC	CACCTCCGCGAGGAGAAAGT	GACGACGACGTCTTGTTCCAC
HNF4a	GAGCTGCAGATCGATGACAA	TACTGGCGGTCGTTGATGTA
KLF4	TCTCAAGGCACACCTGCGAA	TAGTGCCTGGTCAGTTCATC
LTF	GCATGGGCTAAGGATTTGAA	TCCCAAATTTAGCCTGTTGG
MMP9	TTGACAGCGACAAGAAGTGG	GCCATTCACGTCGTCCTTAT
MPO	TGTTTGAGCAGGTCATGAGG	CCAGATGTCGATGTTGTTGG
MYC	ACTCTGAGGAGGAACAAGAA	TGGAGACGTGGCACCTCTT
NANOG	CTGTGATTTGTGGGCCTGAA	TGTTTGCCTTTGGGACTGGT
OCT3/4	AGCGAACCAGTATCGAGAAC	TTACAGAACCACACTCGGAC
PFK1	ATGTGGGTGCCAAAGTCTTC	CAGCTGGATGATGTTGGAGA
PGMase	GTTAAGACCCAGGCGTACCA	GAAGTTCTCCGCGTAGTTGG
PU.1	CCAGCTCAGATGAGGAGGAG	CAGGTCCAACAGGAACTGGT
REX1	TCGCTGAGCTGAAACAAATG	CCCTTCTTGAAGGTTTACAC
RUNX1	CCCTAGGGGATGTTCCAGAT	TGAAGCTTTTCCCTCTTCCA
SOX2	ACACCAATCCCATCCACACT	GCAAACTTCCTGCAAAGCTC
SOX17	TGCAGGCCAGAAGCAGTGTTAC	CCCAAACTGTTCAAGTGGCAGA
TAT	ATCTCTGTTATGGGGCGTTG	TGATGACCACTCGGATGAAA
ZIC1	ACCCCAAAAAGTCGTGCAAC	TTTGGCTTTGAAGGGCTTGC

culture fluid was sampled at the indicated time intervals. Lactic acid was quantitated using a kit according to the manufacturer's instructions.

In the galactose administration assay, iPS-derived hepatocytes were cultured for 30 min in DMEM glucose-free medium containing 2 mM L-glutamine and 0.5% BSA. After 30 min, galactose was added to the medium to adjust the final concentration to 10 mM. The culture fluid was sampled at the indicated time intervals. Lactic acid was quantitated using a kit according to the manufacturer's instructions.

The cells (1-well/24-well dish) were homogenized in 100 μL lysis buffer solution, vortexed and then centrifuged. The resulting supernatants were transferred to fresh tubes to remove debris and insoluble material. For each assay, sample extracts were transferred to a 96-well plate according to the manufacturer's instructions. Then, sample and reaction mix were reacted for 30 min. After 30 min, the sample fluorescence was assayed using a micro plate reader.

Zymosan uptake assay for phagocytic capacity

Cells were suspended in 100 μL of MEMα medium and then incubated with Alexa Fluor 488-conjugated zymosan A for 30 min in a water bath at 37 °C. Cells were then washed with PBS, centrifuged at 350× *g* for 5 min and observed using a fluorescence microscope.

Assay of superoxide anion production

Superoxide production was detected using the fluorescence dye dihydroethidium. Neutrophils derived from iPSCs (1 × 104 cells) were incubated for 30 min in the presence of dihydroethidium and measured using a plate reader with fluorescence emission at λex/λem = 544/612. Images were obtained using a fluorescence microscope. The orange fluorescence of oxidized dihydroethidium was visualized using simultaneous excitation at 518 and 605 nm.

Cells were pre-incubated with the superoxide-sensitive chemiluminescent dye L-012. The L-012 assay mixture contained 50 mM phosphate buffer (pH 7.8), 1 mM EGTA, 0.15 M sucrose and 0.1 mM L-012. The rate of superoxide anion production was measured using a luminometer. Results were standardized to the total protein content.

Evaluation of apoptosis

The activities of caspase-3 and caspase-9 were measured using kits according to manufacturer's instructions. These measurements were based on spectrophotometric detection of the chromophore *p*-nitroanilide (*p*NA) after cleavage from the labeled substrates DEVD-*p*NA or LEHD-*p*NA. Absorbance of *p*NA was quantified using a microtiter plate reader at 405 nm.

Apoptosis was also detected by phosphatidylserine exposure of the plasma membrane surface. Cells were suspended in MEMα culture medium containing annexin V-FITC and incubated for 30 min at 37 °C under a humidified atmosphere of 5% CO_2 and 95% air. After 30 min, neutrophils derived from iPSCs (1 × 104 cells) were measured on a plate reader with fluorescence at λex/λem = 485/538. The FITC fluorescence was also visualized by simultaneous excitation at 488 and 530 nm using a fluorescence microscope. The green fluorescence of FITC was also visualized with simultaneous excitation at 488 and 530 nm using fluorescence microscope. Apoptotic cells were identified on the basis of phosphatidylserine exposure on the plasma membrane surface and on morphologic changes.

Protein assay

Protein assays were carried out using kits according to the manufacturer's instructions. In brief, 160-μL sample solutions were added to the wells of a 96-well plate, and 40 μL of dye reagent concentrate was added to each well. The sample and reagent were mixed thoroughly and were incubated at room temperature for 5 min. Sample absorbance was then measured at 595 nm.

Statistical analyses

All of the measurement results were expressed as mean ± standard errors (SE). Welch's *t*-test was used for analysis between two independent groups. Sheffe's *F*-test was used for comparisons between multiple groups after confirming significance in the analysis of variance. Differences were considered statistically significant when *P*-values were <0.05.

Author contributions

Daisuke Satoh and Tamihide Matsunaga involved in the conception and design. Daisuke Satoh, Thoru Maeda, Mariko Ohte, Akane Ukai, Katsunori Nakamura and Tamihide Matsunaga provided administrative support. Tetsuya Ito, Yoko Nakajima, Shin Enosawa, Masashi Toyota, Yoshitaka Miyagawa, Hajime Okita, Nobutaka Kiyokawa, Hidenori Akutsu and Akihiro Umezawa involved in the provision of study material or patients. Daisuke Satoh, Mariko Ohte and Akane Ukai collected and/or assembled the data. Daisuke Satoh, Mariko Ohte and Akane Ukai analyzed and interpreted the data. Daisuke Satoh wrote the manuscript. Tamihide Matsunaga approved the final manuscript. Tetsuya Ito and Yoko Nakajima are attending physicians. Tetsuya Ito, Yoko Nakajima and Shin Enosawa took the informed consent. Masashi Toyota, Yoshitaka Miyagawa, Hajime Okita, Nobutaka Kiyokawa, Hidenori Akutsu and Akihiro Umezawa established and offered control iPSCs. No financial support was provided for this study.

References

Asahina, K., Fujimori, H., Shimizu-Saito, K., Kumashiro, Y., Okamura, K., Tanaka, Y., Teramoto, K., Arii, S. & Teraoka, H. (2004) Expression of the liver-specific gene Cyp7a1 reveals hepatic differentiation in embryoid bodies derived from mouse embryonic stem cells. *Genes Cells* **9**, 1297–1308.

Berk, P.D. & Stremmel, W. (1986) Hepatocellular uptake of organic anions. *Prog. Liver Dis.* **8**, 125–144.

Borregaard, N., Theilgaard-Mönch, K., Sorensen, O.E. & Cowland, J.B. (2001) Regulation of human neutrophil granule protein expression. *Curr. Opin. Hematol.* **8**, 23–27.

Carvajal-Vergara, X., Sevilla, A., D'Souza, S.L., *et al.* (2010) Patient-specific induced pluripotent stem-cell-derived models of LEOPARD syndrome. *Nature* **465**, 808–812.

Cheung, Y.Y., Kim, S.Y., Yiu, W.H., Pan, C.J., Jun, H.S., Ruef, R.A., Lee, E.J., Westphal, H., Mansfield, B.C. & Chou, J.Y. (2007) Impaired neutrophil activity and increased susceptibility to bacterial infection in mice lacking glucose-6-phosphatase-β. *J. Clin. Invest.* **117**, 784–793.

Chou, J.Y. (1988) Regulators of fetal liver differentiation in vitro. *Arch. Biochem. Biophys.* **263**, 378–386.

Chou, J.Y., Jun, H.S. & Mansfield, B.C. (2010) Neutropenia in type Ib glycogen storage disease. *Curr. Opin. Hematol.* **17**, 36–42.

Chou, J.Y. & Mansfield, B.C. (2011) Recombinant AAV-directed gene therapy for type I glycogen storage diseases. *Expert Opin. Biol. Ther.* **11**, 1011–1024.

Correia, C.E., Bhattacharya, K., Lee, P.J., Shuster, J.J., Theriaque, D.W., Shankar, M.N., Smit, G.P. & Weinstein, D.A. (2008) Use of modified cornstarch therapy to extend fasting in glycogen storage disease types Ia and Ib. *Am. J. Clin. Nutr.* **88**, 1272–1276.

Cowland, J.B. & Borregaard, N. (1999) The individual regulation of granule protein mRNA levels during neutrophil maturation explains the heterogeneity of neutrophil granules. *J. Leukoc. Biol.* **66**, 989–995.

Czop, J.K. (1986) The role of beta-glucan receptors on blood and tissue leukocytes in phagocytosis and metabolic activation. *Pathol. Immunopathol. Res.* **5**, 286–296.

Dimos, J.T., Rodolfa, K.T., Niakan, K.K., Weisenthal, L.M., Mitsumoto, H., Chung, W., Croft, G.F., Saphier, G., Leibel, R., Goland, R., Wichterle, H., Henderson, C.E. & Eggan, K. (2008) Induced pluripotent stem cells generated from patients with ALS can be differentiated into motor neurons. *Science* **321**, 1218–1221.

Dissanayake, V.H., Jayasinghe, J.D., Thilakaratne, V. & Jayasekara, R.W. (2010) Novel mutation in SLC37A4 gene in a Sri Lankan boy with glycogen storage disease type Ib associated with very early onset neutropenia. *J. Mol. Genet. Med.* **5**, 262–263.

Donadieu, J., Fenneteau, O., Beaupain, B., Mahlaoui, N. & Chantelot, C.B. (2011) Congenital neutropenia: diagnosis, molecular bases and patient management. *Orphanet J. Rare Dis.* **6**, 26.

Fasske, E. & Morgenroth, K. (1985) Functional morphology of phagocytosing alveolar macrophages. Long-term electron microscopic and X-ray microanalytical investigations on the rat model. *Virchows Arch. B Cell Pathol. Incl. Mol. Pathol.* **49**, 195–208.

Fernandes, J., Koster, J.F., Grose, W.F. & Sorgedrager, N. (1974) Hepatic phosphorylase deficiency. Its differentiation from other hepatic glycogenoses. *Arch. Dis. Child.* **49**, 186–191.

Friedman, A.D. (2007) Transcriptional control of granulocyte and monocyte development. *Oncogene* **26**, 6816–6828.

Guionie, O., Clottes, E., Stafford, K. & Burchell, A. (2003) Identification and characterization of a new human glucose-6-phosphatase isoform. *FEBS Lett.* **551**, 159–164.

Kasahara, M., Horikawa, R., Sakamoto, S., Shigeta, T., Tanaka, H., Fukuda, A., Abe, K., Yoshii, K., Naiki, Y., Kosaki, R. & Nakagawa, A. (2009) Living donor liver transplantation for glycogen storage disease type Ib. *Liver Transpl.* **15**, 1867–1871.

Kim, S.Y., Jun, H.S., Mead, P.A., Mansfield, B.C. & Chou, J.Y. (2008) Neutrophil stress and apoptosis underlie myeloid dysfunction in glycogen storage disease type Ib. *Blood* **111**, 5704–5711.

Kuijpers, T.W., Maianski, N.A., Tool, A.T., Smit, G.P., Rake, J.P., Roos, D. & Visser, G. (2003) Apoptotic neutrophils in the circulation of patients with glycogen storage disease type 1b (GSD1b). *Blood* **101**, 5021–5024.

Lanier, L.L., Phillips, J.H., Testi, R. (1989) Membrane anchoring and spontaneous release of CD16 (FcR III) by natural killer cells and granulocytes. *Eur. J. Immunol.* **19**, 775–778.

Lee, G., Papapetrou, E.P., Kim, H., Chambers, S.M., Tomishima, M.J., Fasano, C.A., Ganat, Y.M., Menon, J., Shimizu, F., Viale, A., Tabar, V., Sadelain, M. & Studer, L. (2009) Modelling pathogenesis and treatment of familial dysautonomia using patient-specific iPSCs. *Nature* **461**, 402–406.

Li, P., Nijhawan, D., Budihardjo, I., Srinivasula, S.M., Ahmad, M., Alnemri, E.S. & Wang, X. (1997) Cytochrome c and dATP-dependent formation of Apaf-1/caspase-9 complex initiates an apoptotic protease cascade. *Cell* **91**, 479–489.

Maehr, R., Chen, S., Snitow, M., Ludwig, T., Yagasaki, L., Goland, R., Leibel, R.L. & Melton, D.A. (2009) Generation of pluripotent stem cells from patients with type 1 diabetes. *Proc. Natl Acad. Sci. USA* **106**, 15768–15773.

Melis, D., Della-Casa, R., Parini, R., Rigoldi, M., Cacciapuoti, C., Marcolongo, P., Benedetti, A., Gaudieri, V., Andria, G. & Parenti, G. (2008) Vitamin E supplementation improves neutropenia and reduces the frequency of infections in patients with glycogen storage disease type 1b. *Eur. J. Pediatr.* **168**, 1069–1074.

Melis, D., Parenti, G., Della-Casa, R., Sibilio, M., Berni-Canani, R., Terrin, G., Cucchiara, S. & Andria, G. (2003) Crohn's like ileo-colitis in patients affected by glycogen storage disease Ib: two years' follow-up of patients with a wide spectrum of gastrointestinal signs. *Acta Paediatr.* **92**, 1415–1421.

Melis, D., Pivonello, R., Parenti, G., Della-Casa, R., Salerno, M., Lombardi, G., Sebastio, G., Colao, A. & Andria, G. (2007) Increased prevalence of thyroid autoimmunity and hypothyroidism in patients with glycogen storage disease type I. *J. Pediatr.* **150**, 300–305.

Morishima, T., Watanabe, K., Niwa, A., Fujino, H., Matsubara, H., Adachi, S., Suemori, H., Nakahata, T. & Heike, T. (2011) Neutrophil differentiation from human-induced pluripotent stem cells. *J. Cell. Physiol.* **226**, 1283–1291.

Muller, M. & Jansen, P.L. (1998) The secretory function of the liver: New aspects of hepatobiliary transport. *J. Hepatol.* **28**, 344–354.

Narisawa, K., Igarashi, Y., Otomo, H. & Tada, K. (1978) A new variant of glycogen storage disease type I probably due to a defect in the glucose-6-phosphate transport system. *Biochem. Biophys. Res. Commun.* **83**, 1360–1364.

Okabayashi, K. & Asashima, M. (2003) Tissue generation from amphibian animal caps. *Curr. Opin. Genet. Dev.* **13**, 502–507.

Park, I.H., Arora, N., Huo, H., Maherali, N., Ahfeldt, T., Shimamura, A., Lensch, M.W., Cowan, C., Hochedlinger, K. & Daley, G.Q. (2008) Disease-specific induced pluripotent stem (iPS) cells. *Cell* **134**, 877–886.

Pulido, R., Lacal, P., Mollinedo, F. & Sánchez-Madrid, F. (1989) Biochemical and antigenic characterization of CD45 polypeptides expressed on plasma membrane and internal granules of human neutrophils. *FEBS Lett.* **249**, 337–342.

Rashid, S.T., Corbineau, S., Hannan, N., Marciniak, S.J., Miranda, E., Alexander, G., Huang-Doran, I., Griffin, J., Ahrlund-Richter, L., Skepper, J., Semple, R., Weber, A., Lomas, D.A. & Vallier, L. (2010) Modeling inherited metabolic disorders of the liver using human induced pluripotent stem cells. *J. Clin. Invest.* **120**, 3127–3136.

Raya, A., Rodríguez-Pizà, I., Guenechea, G., *et al.* (2009) Disease-corrected haematopoietic progenitors from Fanconi anaemia induced pluripotent stem cells. *Nature* **460**, 53–59.

Sakai, K., Hattori, T., Sagawa, K., Yokoyama, M. & Takatsuki, K. (1987) Biochemical and functional characterization of MCS-2 antigen (CD13) on myeloid leukemic cells and polymorphonuclear leukocytes. *Cancer Res.* **47**, 5572–5576.

Scott, F.L., Denault, J.B., Riedl, S.J., Shin, H., Renatus, M. & Salvesen, G.S. (2005) XIAP inhibits caspase-3 and -7

using two binding sites: evolutionarily conserved mechanism of IAPs. *EMBO J.* **24**, 645–655.

Soldner, F., Hockemeyer, D., Beard, C., Gao, Q., Bell, G.W., Cook, E.G., Hargus, G., Blak, A., Cooper, O., Mitalipova, M., Isacson, O. & Jaenisch, R. (2009) Parkinson's disease patient-derived induced pluripotent stem cells free of viral reprogramming factors. *Cell* **136**, 964–977.

Takahashi, K., Tanabe, K., Ohnuki, M., Narita, M., Ichisaka, T., Tomoda, K. & Yamanaka, S. (2007) Induction of pluripotent stem cells from adult human fibroblasts by defined factors. *Cell* **13**, 861–872.

Tsuchiya, H., Matsunaga, T., Aikawa, K., Kamada, N., Nakamura, K., Ichikawa, H., Sasaki, K. & Ohmori, S. (2012) Evaluation of human embryonic stem cell-derived hepatocyte-like cells for detection of CYP1A inducers. *Drug Metab. Pharmacokinet.* **27**, 598–604.

Visser, G., de Jager, W., Verhagen, L.P., Smit, G.P., Wijburg, F.A., Prakken, B.J., Coffer, P.J. & Buitenhuis, M. (2012) Survival, but not maturation, is affected in neutrophil progenitors from GSD-1b patients. *J. Inherit. Metab. Dis.* **35**, 287–300.

Yamada, T., Yoshikawa, M., Kanda, S., Kato, Y., Nakajima, Y., Ishizaka, S. & Tsunoda, Y. (2002) In vitro differentiation of embryonic stem cells into hepatocyte-like cells identified by cellular uptake of indocyanine green. *Stem Cells* **20**, 146–154.

Ye, L., Chang, J.C., Lin, C., Sun, X., Yu, J. & Kan, Y.W. (2009) Induced pluripotent stem cells offer new approach to therapy in thalassemia and sickle cell anemia and option in prenatal diagnosis in genetic diseases. *Proc. Natl. Acad. Sci. USA* **106**, 9826–9830.

Yiu, W.H., Pan, C.J., Allamarvdasht, M., Kim, S.Y. & Chou, J.Y. (2007) Glucose-6-phosphate transporter gene therapy corrects metabolic and myeloid abnormalities in glycogen storage disease type Ib mice. *Gene Ther.* **14**, 219–226.

Yiu, W.H., Pan, C.J., Mead, P.A., Starost, M.F., Mansfield, B.C. & Chou, J.Y. (2009) Normoglycemia alone is insufficient to prevent long term complications of hepatocellular adenoma in glycogen storage disease type Ib mice. *J. Hepatol.* **51**, 909–917.

Yu, J., Vodyanik, M.A., Smuga-Otto, K., Antosiewicz-Bourget, J., Frane, J.L., Tian, S., Nie, J., Jonsdottir, G.A., Ruotti, V., Stewart, R., Slukvin, I.I. & Thomson, J.A. (2007) Induced pluripotent stem cell lines derived from human somatic cells. *Science* **318**, 1917–1920.

Received: 26 May 2013
Accepted: 22 August 2013

Supporting Information

Additional Supporting Information may be found in the online version of this article at the publisher's web site:

Figure S1 Generation of induced pluripotent stem cells (iPSCs) derived from a patient with glycogen storage disease type Ib (GSDIb).

Figure S2 Analysis of embryoid body (EB) formation.

Figure S3 *In vitro* differentiation of induced pluripotent stem cells (iPSCs) derived from a patient with glycogen storage disease type Ib.

Figure S4 Expression of hepatocyte markers on day 25.

Figure S5 Quantitative polymerase chain reaction analysis of expression of genes marking key stages of induced pluripotent stem cell (iPSC) differentiation.

LIVER TRANSPLANTATION 20:391–393, 2014

LETTER FROM THE FRONTLINE

Hepatocyte Transplantation Using a Living Donor Reduced Graft in a Baby With Ornithine Transcarbamylase Deficiency: A Novel Source of Hepatocytes

Received October 29, 2013; accepted November 17, 2013.

TO THE EDITORS:

We performed hepatocyte transplantation (HT) in an 11-day-old infant with ornithine transcarbamylase deficiency (OTCD). We used cryopreserved hepatocytes prepared from remnant liver tissue, a byproduct of a hyper-reduced left lateral segment from living donor liver transplantation (LDLT). The patient exhibited hypothermia, drowsiness, and apnea at 3 days of age; these symptoms were accompanied by hyperammonemia (1940 μg/dL at maximum), although there were no abnormalities at birth or an obvious family history (Fig. 1). Further examinations confirmed that the hyperammonemia was the result of OTCD. Multimodal treatments, including alimentotherapy, medications, and continuous hemodiafiltration (CHDF), did not improve the patient's clinical state, and severe hyperammonemia attacks recurred. Because of the patient's small body size (2550 g) and the lack of an available liver donor, HT was indicated. Hepatocytes of the same blood type were chosen from an institutional repository of cryopreserved hepatocytes prepared from the remnant tissue of segment III from unrelated living donors. Thawed hepatocytes were transplanted twice at 11 and 14 days of age with a double-lumen catheter inserted into the left portal vein via the umbilical vein (Fig. 2). The amounts of transplanted hepatocytes were 7.4×10^7 and 6.6×10^7 cells/body, and the viability rates were 89.1% and 82.6%, respectively. The portal flow was kept stable at greater than 10 mL/kg/minute, and the pressure was maintained at less than 20 mm Hg during and after HT. The immunosuppressive treatment followed the same protocol used for LDLT with tacrolimus and low-dose steroids.[1] The patient was weaned from CHDF and the ventilator at 26 and 30 days of age, respectively, with a stable serum ammonia level of 40 μg/dL. The patient was ultimately discharged 56 days after HT. During the 3 months of follow-up, the baby did well with protein restriction (2 g/kg/day), medication for OTCD, and immunosuppression. No neurological sequelae related to hyperammonemia have been observed so far (Fig. 1).

DISCUSSION

For children with metabolic liver disease, HT is indicated as an alternative or bridge to liver transplantation.[2] HT is less invasive than liver transplantation and can be performed repeatedly. Limitations to the widespread application of HT include the poor availability of hepatocytes. Therefore, it is important to find new sources of high-quality hepatocytes. We previously prepared a repository of hepatocytes obtained from remnant liver tissue, a byproduct of hyper-reduced left lateral segmentectomy in LDLT.[1]

The cell donor was an unrelated volunteer with the same blood type who had previously undergone hyper-reduced left lateral segmentectomy. The main unit of segment II was used as a monosegmental liver graft for the primary recipient with end-stage liver disease, and the remnant was used to isolate hepatocytes with fully informed consent. The hepatocytes were isolated according to the collagenase perfusion method, as described elsewhere,[3] with Liberase MTF C/T GMP grade (Roche). All procedures were performed at our cell processing center according to a strictly controlled protocol based on good manufacturing practices. The total number of transplanted live hepatocytes was 1.4×10^8 cells/body; the ammonia removal rate was more than 200 fmol/cell/hour (203.4 and 265.4 fmol/cell/hour with the first and second injections, respectively). The dose was judged to be sufficiently high to obtain therapeutic effectiveness according to our theoretical background.[4]

This work was supported by a grant-in-aid from the National Center for Child Health and Development and the Highway Program for the Realization of Regenerative Medicine (Japanese Science and Technology Agency). This study protocol was approved by institutional review board in National Center for Child Health and Development (reference number 433).

Address reprint requests to Mureo Kasahara, M.D., Ph.D., National Center for Child Health and Development, 2-10-1 Okura, Setagaya-Ku, Tokyo, Japan 157-8535. Telephone: +81-3-3416-0181; FAX: +81-3-3416-2222; E-mail: kasahara-m@ncchd.go.jp

DOI 10.1002/lt.23800
View this article online at wileyonlinelibrary.com.
LIVER TRANSPLANTATION. DOI 10.1002/lt. *Published on behalf of the American Association for the Study of Liver Diseases*

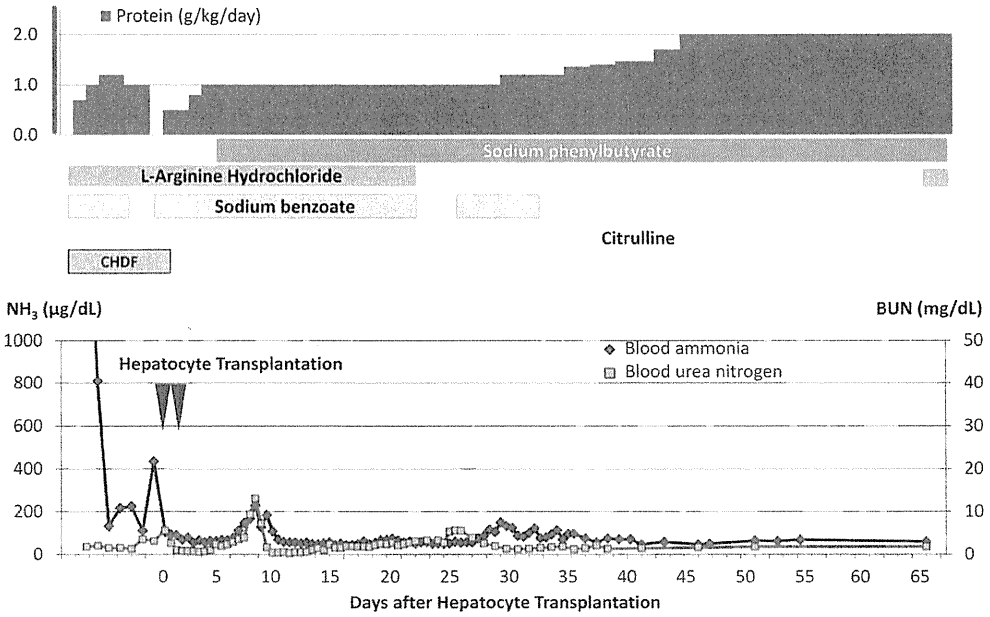

Figure. 1. Treatment schedule (top) and patient condition (bottom). The changes with time for blood ammonia and blood urea nitrogen are shown. The baby was delivered vaginally as a first child. At 3 days of age, hypothermia, low oxygen saturation, and, finally, respiratory arrest occurred. The patient was incubated and given artificial respiration. Concurrently, hyperammonemia (1940 μg/dL) was found, and continuous hemodiafiltration (CHDF) was started in addition to alimentotherapy (protein withdrawal) and medications. Whenever the administration of essential amino acids was restarted, the blood ammonia level became elevated, and at 9 days of age, despite the suspension of essential amino acid administration, the level increased up to 434 μg/dL. At 11 days of age, HT was performed for the first time, and it was performed for the second time at 14 days of age. After HT, amino acid intake was restarted along with the continuation of multimodal treatments, and blood ammonia was controlled well except for episodic increases. The patient was weaned from CHDF and the ventilator at 26 and 30 days of age, respectively, and the patient was ultimately discharged 56 days after HT.

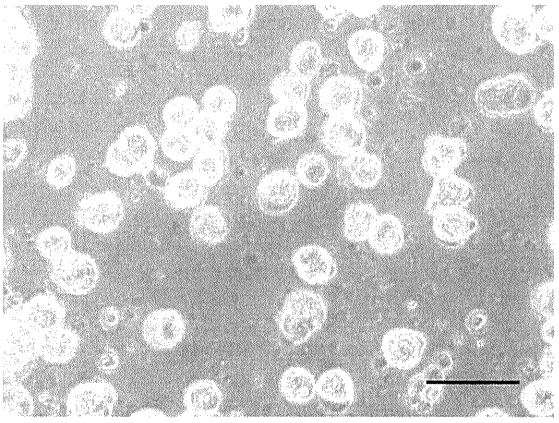

Figure. 2. Hepatocytes transplanted during the first injection. The cells showed a glazed and firm surface. The bar indicates 50 μm.

Because liver transplantation is approved as a treatment for end-stage hepatic failure, donor livers are preferentially allocated for organ transplantation and not for hepatocyte isolation. On rare occasions, the lack of appropriate donor-recipient matching (eg, infant donor livers) provides good-quality hepatocytes.[2] Fetal livers are also considered to be an alternative cell source, although ethical issues remain to be resolved. At present, we have little choice but to use marginal donor tissues, such as livers obtained from donors after cardiac death and organs with steatosis, fibrosis, or a long ischemia time. However, there are unfavorable issues related to the use of marginal donors, including low viability and vulnerability to cryopreservation. In this respect, the remnant liver tissue of hyper-reduction procedures used in LDLT has the same quality as that of left lateral segment grafts. As for availability, there are 5 cases of hyper-reduction per year at our institution on average.[5] The use of remnant liver tissues obtained from hyper-reduced LDLT procedures will, therefore, help to address the shortage of hepatocyte donors.

Shin Enosawa, D.D.S., Ph.D.
Reiko Horikawa, M.D., Ph.D.
Akiko Yamamoto, M.D.
Seisuke Sakamoto, M.D., Ph.D.
Takanobu Shigeta, M.D.
Shunsuke Nosaka, M.D., Ph.D.
Junichiro Fujimoto, M.D., Ph.D.
Atsuko Nakazawa, M.D., Ph.D.
Akito Tanoue, M.D., Ph.D.
Kazuaki Nakamura, Ph.D.
Akihiro Umezawa, M.D., Ph.D.
Yoichi Matsubara, M.D., Ph.D.
Akira Matsui, M.D., Ph.D.
Mureo Kasahara, M.D., Ph.D.
National Center for Child Health and Development, Tokyo, Japan

REFERENCES

1. Kasahara M, Kaihara S, Oike F, Ito T, Fujimoto Y, Ogura Y, et al. Living-donor liver transplantation with monosegments. Transplantation 2003;76:694-696.
2. Meyburg J, Das AM, Hoerster F, Lindner M, Kriegbaum H, Engelmann G, et al. One liver for four children: first clinical series of liver cell transplantation for severe neonatal urea cycle defects. Transplantation 2009;87:636-641.
3. Alexandrova K, Griesel C, Barthold M, Heuft HG, Ott M, Winkler M, et al. Large-scale isolation of human hepatocytes for therapeutic application. Cell Transplant 2005; 14:845-853.
4. Enosawa S, Yuan W, Douzen M, Nakazawa A, Omasa T, Fukuda A, et al. Consideration of a safe protocol for hepatocyte transplantation using infantile pigs. Cell Med 2012;3:13-18.
5. Kanazawa H, Sakamoto S, Fukuda A, Uchida H, Hamano I, Shigeta T, et al. Living-donor liver transplantation with hyperreduced left lateral segment grafts: a single-center experience. Transplantation 2013;95: 750-754.

Kami et al. BMC Biotechnology 2013, 13:102
http://www.biomedcentral.com/1472-6750/13/102

BMC Biotechnology

RESEARCH ARTICLE Open Access

Large-scale cell production of stem cells for clinical application using the automated cell processing machine

Daisuke Kami[1], Keizo Watakabe[2], Mayu Yamazaki-Inoue[3], Kahori Minami[3], Tomoya Kitani[4], Yoko Itakura[5], Masashi Toyoda[5], Takashi Sakurai[2], Akihiro Umezawa[3] and Satoshi Gojo[1*]

Abstract

Background: Cell-based regeneration therapies have great potential for application in new areas in clinical medicine, although some obstacles still remain to be overcome for a wide range of clinical applications. One major impediment is the difficulty in large-scale production of cells of interest with reproducibility. Current protocols of cell therapy require a time-consuming and laborious manual process. To solve this problem, we focused on the robotics of an automated and high-throughput cell culture system. Automated robotic cultivation of stem or progenitor cells in clinical trials has not been reported till date. The system AutoCulture® used in this study can automatically replace the culture medium, centrifuge cells, split cells, and take photographs for morphological assessment. We examined the feasibility of this system in a clinical setting.

Results: We observed similar characteristics by both the culture methods in terms of the growth rate, gene expression profile, cell surface profile by fluorescence-activated cell sorting, surface glycan profile, and genomic DNA stability. These results indicate that AutoCulture® is a feasible method for the cultivation of human cells for regenerative medicine.

Conclusions: An automated cell-processing machine will play important roles in cell therapy and have widespread use from application in multicenter trials to provision of off-the-shelf cell products.

Keywords: Automated cell culture system, Cell transplantation, Stem cells, Clinical trial, Cell processing facility

Background

Degenerative diseases affect increasing numbers of people, particularly in developed countries with aging populations. Despite advancements in medicine, modalities to cure advanced diseases are often not available. Therefore, regenerative therapy may become the standard treatment option in cardiovascular medicine. Recent developments in stem cell biology, including those related to induced pluripotent stem cells (iPSCs) and tissue-derived stem/progenitor cells, are a giant leap toward the goal. Recently, myocardium-derived stem/progenitor cells were isolated by several institutes [1-3]. These cell populations have the potential to repair the diseased heart, and clinical trials are currently ongoing.

In tandem with these developments in stem cell biology and the large number of completed and ongoing clinical trials, attempts have been made to commercialize these therapies [4]. The most prominent therapeutic strategy is cell transplantation. However, harvested cells or tissues are usually limited in quantity and stem cells properties may vary from batch to batch, hindering the reliability for clinical applications. Moreover, current cell therapy protocols are laboratory centered and labor intensive, requiring highly skilled personnel and weeks to months to harvest sufficient quantities of stem/progenitor cells from the isolated tissues. These manual procedures are expensive and can result in high phenotypic and yield variability between different trials and institutions [5].

Strategies to validate advanced medicinal products have been established; however, these "best practices" still depend on the ability of personnel to perform them, such as the cultivation of stem/progenitor cells under strictly

* Correspondence: gojos@koto.kpu-m.ac.jp
[1]Department of Regenerative Medicine, Kyoto Prefectural University of Medicine, 465 Kajii-cho, Kawaramachi-Hirokoji, Kamigyo-ku, Kyoto 602-8566, Japan
Full list of author information is available at the end of the article

controlled conditions [6]. High process reproducibility can be achieved by automation, and several effective automatic cell culture systems have been reported [7-12]. These automated platforms have the potential to provide cost-effective, large-scale expansion of stem/progenitor cells with consistent phenotype for clinical use and improved operational safety [13]. Progress in robot platforms for cell culture has resulted in several prototypes to implement large-scale expansion and harvesting of stem/progenitor cells with yield and phenotypic reproducibility. An automated culture system by "The Automation Partnership Biosystems (TAP Biosystems)" has cultivated human embryonic stem cells and bone marrow-derived cells [14,15]. Kawasaki Heavy Industries (Tokyo, Japan) has created AutoCulture® (Additional file 1), which can automate many manual steps in cell culture, including media exchange, centrifugation of cells, splitting and passaging, and recording of cell morphology (Figure 1A). To the best of our knowledge, no cell products obtained from an automated culture apparatus have actually been transplanted into humans for regenerative therapy.

Our institute recently completed a phase I clinical trial using autologous cardiac stem cells (CSCs) isolated by manual cell culture techniques to treat ischemic cardiomyopathy [16]. The trial is registered in the Japanese government database for clinical trials using human stem cells and ClinicalTrials.gov, which is a world-wide registry and results database for clinical trials involving humans, as AutoLogous Human CArdiac-Derived Stem Cell to Treat Ischemic cArdiomyopathy (ALCADIA; Identifier: NCT00981006). CSCs are manually cultivated by a single experienced investigator for approximately 1 month to minimize variability of the final cell products. To advance this trial from a single-center to a multi-center randomized trial, we evaluated AutoCulture® by comparing the growth rate, morphology, and phenotype of cells cultivated using this method with those of manually cultured CSCs.

Results

Cellular morphology and growth

Calculations based on the net cell number and doubling time obtained in the ALCADIA trial (Additional file 2)

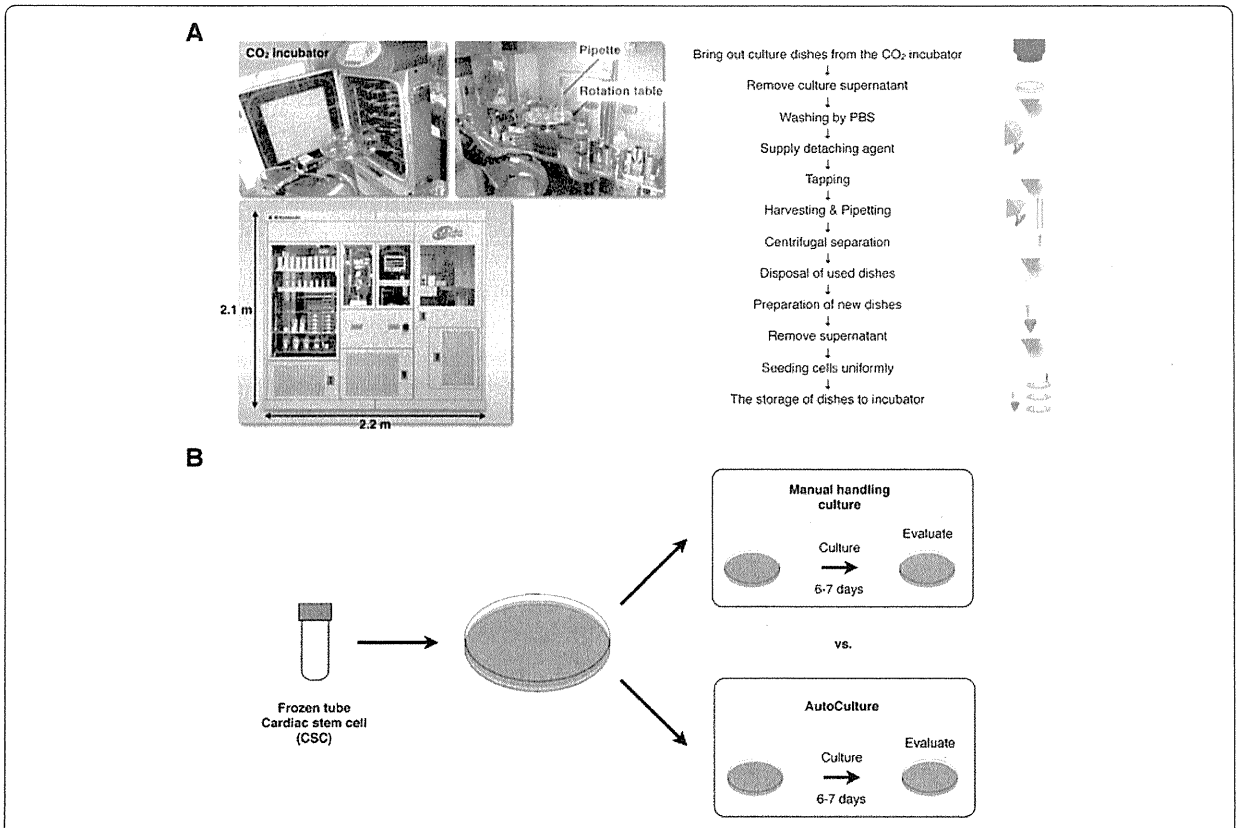

Figure 1 Process maps showing the key steps in human cardiac stem cell culture using manual methods and the AutoCulture® system. **(A)** The automated culture system AutoCulture® by Kawasaki Heavy Industries (left) can automate every step of manual cell culture under current good manufacturing practice (cGMP) grade. **(B)** Schematic representation of the experiment. Human cardiac stem cells (CSCs) were thawed and split into 2 dishes for either manual culture or automated culture using AutoCulture®.

indicated that a culture duration of 2 weeks was sufficient to obtain the appropriate cell number for clinical trial when cells after the second passage (P2) were used as the starting material. Identically seeded culture plates were maintained manually or by automation using AutoCulture® (Figure 1B). The morphology of CSCs cultured using the automated system was similar to that of manually cultured CSCs on day 7 and 14 after seeding (Figure 2A). Under both the conditions, the cells were of similar size, exhibited a low nucleus/cytoplasm ratio, and had a spindle-like shape. In addition, the growth rate was not significantly different, as indicated by cell counts at passage (Figure 2B). Trypan blue staining revealed no significant difference in cell viability between the culture methods. Moreover, both the methods effectively washed out the cells, as indicated by the paucity of adherent cells on discarded culture dishes (data not shown). These results suggest that manual passage was effectively replicated using AutoCulture®.

Gene expression

To investigate the gene expression profiles, RT-PCR analysis was performed according to the shipping criteria for cultivated cells in the current clinical trial (ALCADIA). We examined expression levels of the pluripotency related genes *NANOG*, *OCT4*, *SOX2*, and *REX1* and 2 transcription factor genes involved in cardiomyocyte development, *NKX2.5* and *GATA4* (Figure 2C). The stem cell markers *OCT4*, *REX1*, and *GATA4* were expressed by both cell populations; however, neither *NANOG* nor *NKX2.5* expression was detectable. Moreover, expression levels were not significantly different between the 2 groups on either day 7 or day 14.

Cell surface marker expression profiles

Cell surface markers indicative of CSCs and other phenotypes were detected by fluorescence-activated cell sorting (FACS) (Figure 3A). Under both the culture conditions, the cells were positive for the mesenchymal stem cell (MSC) markers CD29 and CD90 and the vascular endothelial marker CD105 and negative for the hematopoietic lineage marker CD45 and MHC class II. In addition, fluorescent intensities measured by FACS were similar for all positive markers, indicating that equal proportions of cells in both the populations expressed these proteins. Moreover, almost all the cells were CD29 positive, whereas at least 2 populations were distinguished on the basis of CD90 expression. Furthermore, STRO-1, which is expressed by mesenchymal stem cells in the bone marrow, was negative in both the populations. Although the surface expression profiles of CSCs and bone marrow-derived stem cells overlap, STRO-1 expression can discriminate cardiac MSCs from bone marrow-derived MSCs.

Surface glycan expression profile by lectin microarray analysis

Recently, glycan expression profiling has been reported to be an effective cell validation tool to complement phenotype analysis by epigenetic and gene expression analyses

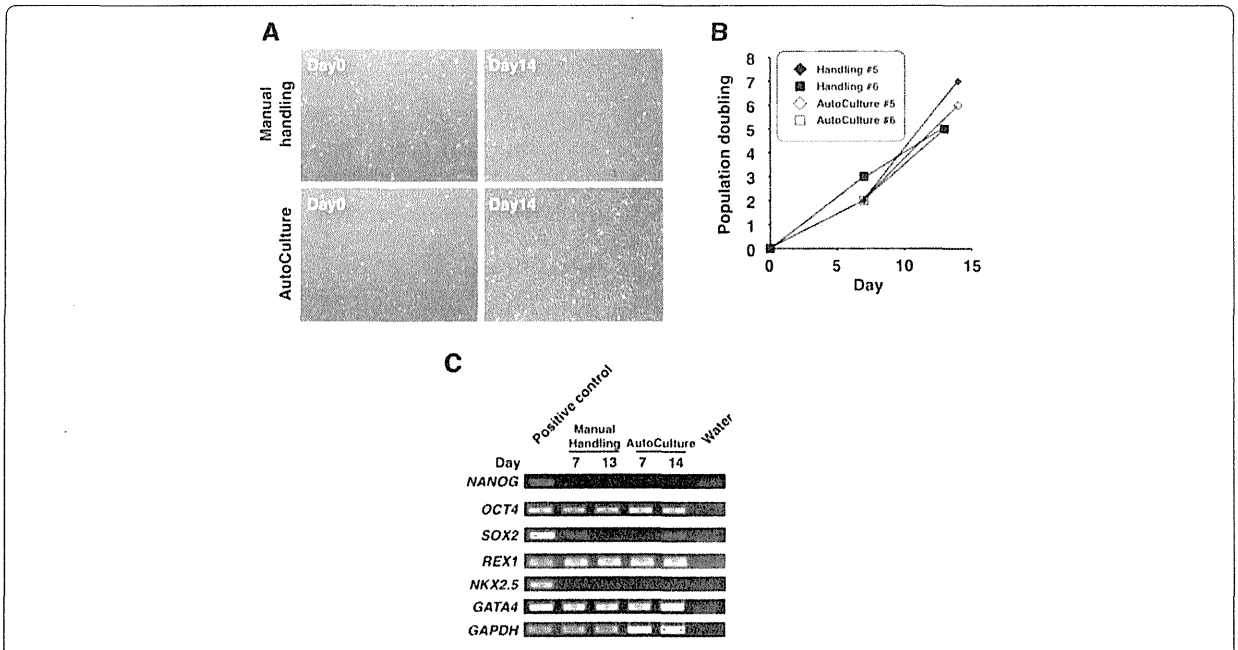

Figure 2 Phenotypic characterizations of CSCs during manual and automated culture. (A) Phase contrast microphotographs of CSCs cultivated either by manual handling (upper panels) or using AutoCulture® (lower panels). **(B)** Growth rates of CSCs under manual or automated culture. **(C)** RT-PCR analysis of genes related to pluripotency and cardiac-specific transcription factors.

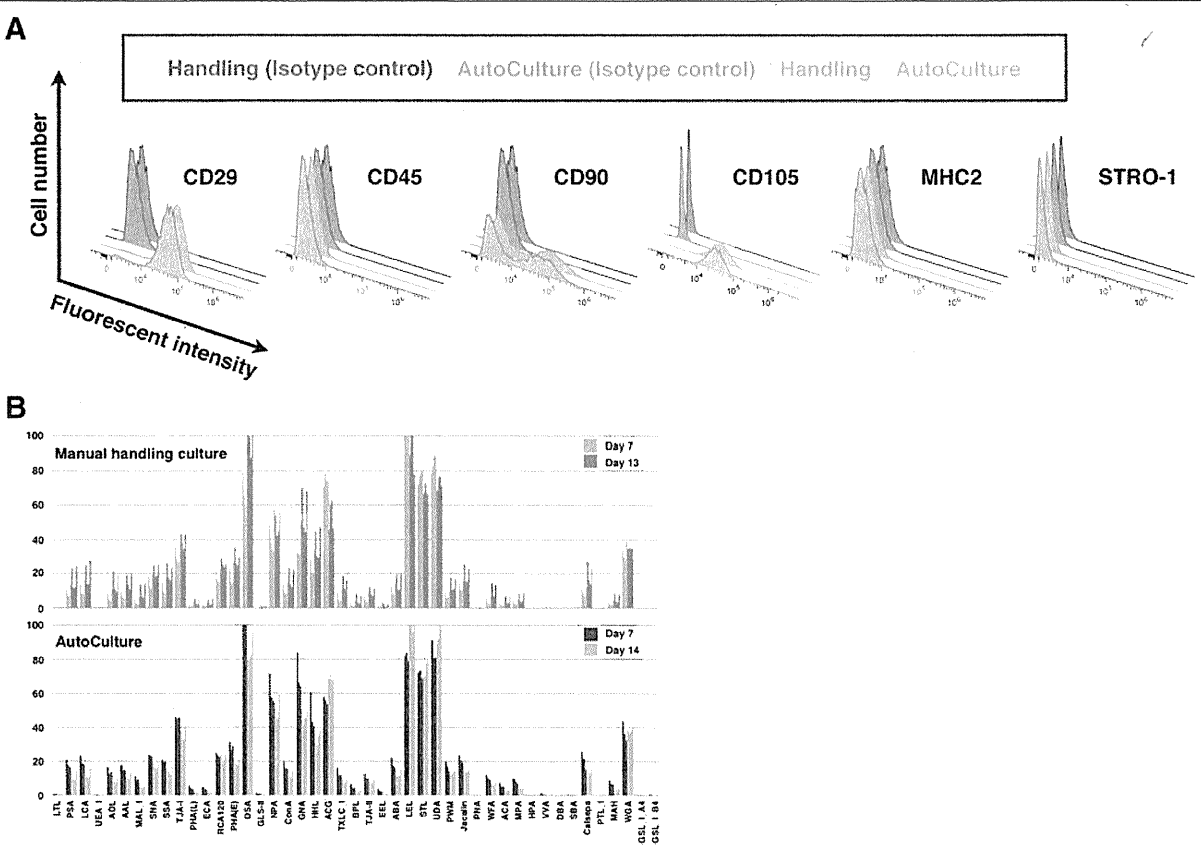

Figure 3 Analysis of cell surface protein and glycan expression in CSCs expanded by manual culture or AutoCulture®. (A) Cells were stained with fluorescence-conjugated primary antibodies and analyzed for surface expression by fluorescence-activated cell sorting. **(B)** Lectin microarray analysis of manual cultures and cells maintained using AutoCulture® on day 7 and day 13/14. The glycan profiles showed little difference between the two culture groups at any time.

[17]. These lectin profiles showed similar patterns, and no significant differences in expression intensities were observed between the 2 culture groups on either day 7 or day 13/14 after seeding (Figure 3B). The washing process used to harvest adherent cells may have profound effects on the cell surface structure and expression. CSCs harvested from the AutoCulture® system exhibited similar surface expression profiles and overall viability to those cultured manually.

Analysis of array comparative genomic hybridization (aCGH) and microarray

To detect genomic DNA mutations on AutoCulture®, we performed aCGH analysis (Agilent technologies) on day 7 and day 14 and compared them with the tissue derived from human right atrial appendage (RAA) (Figure 4A). There were no differences in genomic DNA mutation between CSCs in AutoCulture® and RAA. To investigate the global gene expression profile changes between CSCs in manual culture and CSCs in AutoCulture®, we performed a pairwise comparison of gene expression microarray data using NIA array analysis [18]. The results revealed a similar gene pattern between them (Figure 4B, Additional file 3). The "Symbol" of 162 gene probes was left blank in 258 overexpressed gene probes.

Discussion

Cell-based regenerative medicine is still in the early stages of development [19,20]. The quality of cells for transplant depends on the ability of skilled personnel to isolate, expand, and harvest cultured cells. For consistency of cell yield and phenotype, it is imperative that methodological consistency is strictly maintained. Automation greatly enhances the consistency of culture conditions and may thus reduce the variability in cell quality that is one of the great impediments to the widespread application of cell-based therapy till date. In this study, we used the automated cell culture system AutoCulture® to expand human CSCs isolated from the RAA for use in the ALCADIA clinical trial designed to assess the safety of cell-based therapy for patients with ischemic cardiomyopathy. RAA-derived cells containing CSCs exhibited similar growth rates and gene

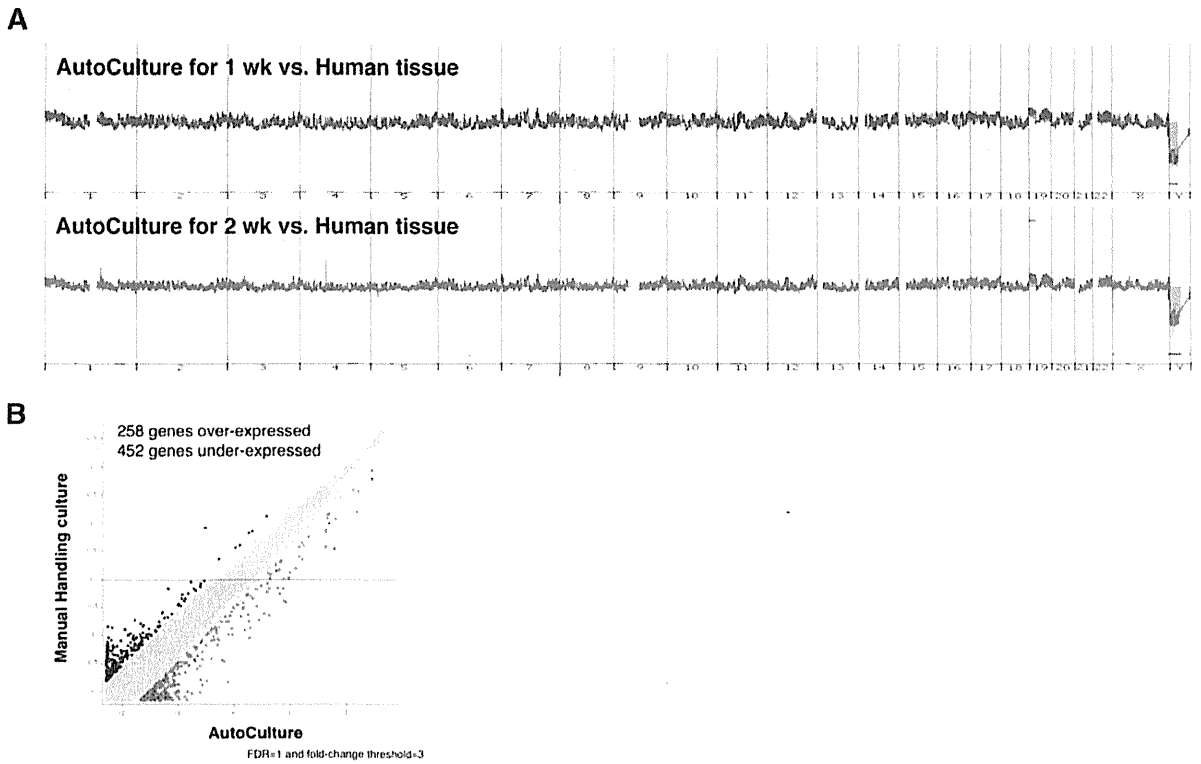

Figure 4 Global analysis of gene expression and genomic DNA mutations. (A) Comparison of array comparative genomic hybridization analysis. Human gDNA (from RAA) was compared to gDNA extracted from CSCs cultivated using AutoCulture® after 1 and 2 weeks using CGH arrays (arrays G4413A). **(B)** Microarray analysis of gene expression profiles. The pairwise scatter plot presents differences in gene expression on day 7 after seeding between manually cultured CSCs and those cultured using AutoCulture®. Grey dots represent transcripts with a subthreshold difference in expression. Red or green dots indicate those with at least a 3-fold difference in expression levels between the two groups. Gene expression levels are depicted on a log2 scale. The number of differentially expressed genes is indicated above.

expression profiles between manual and automated cultures. Thus, the AutoCulture® system effectively replicated manual culture and demonstrated scalability and stability in addition to safety and cost-effectiveness. Indeed, we found no significant differences in phenotype between the two culture methods. Cells in both the populations had similar morphologies, mean growth rates, and expression levels of genes associated with pluripotency and the mesenchymal lineage. In addition, the surface glycan profile was virtually identical, while aCGH analysis revealed no difference in genomic DNA mutation frequency. Finally, the approximately 41,000-probe Agilent Whole Human Genome Microarray chip G4112F showed that only approximately 1% of transcripts measured were significantly under- or overexpressed. The successful transfer of manual to automated cell culture may be attributable to the high flexibility of the machine, which can faithfully copy every step and condition, including media changes, splitting, and passaging in a controlled environment.

AutoCulture® is an all-in-one automated cell culture system consisting of robot arms, tube and flask decappers, flask holders, flask tappers, media pumps, a pipette head, a centrifugal separator, a rotating plate, and a CO_2 incubator. In addition to media change and passage, it permits routine observation. To automate these culture steps, it is necessary to program the humidity, temperature, volume and flow of liquid, and robot arm motion that transfers flasks from or into the CO_2 incubator or flask holder. Another automated cell culture platform, TAP CompacT, was also shown to be an effective system for culture of adherent cells by the Healthcare Engineering group [14]. However, the lack of a centrifugal separator in that system may result in differences between the manual and automated processes, possibly explaining why automation resulted in a smaller population of STRO-1+ cells and overall lower cell yield after the first passage [21]. STRO-1 expression is not a necessary or specific marker for stem or progenitor cells, and somatic stem cells may be more resistant to nutritional and chemical stress [22]. Residual trypsin in the culture media may have adversely affected the survival of differentiated cells, but it is not clear whether stem or progenitor cells can survive or not. On the other hand, the AutoCulture® system efficiently removes trypsin/EDTA by washing and centrifugation. There were no significant

differences in the surface marker expression profile or the mean rate of proliferation between these cells and those maintained manually, strongly suggesting that both populations of RAA-derived CSCs contain equal properties.

The AutoCulture® system can save labor and costs by expanding the scale of production and maintaining uniformity of results. In addition, this system can simultaneously cultivate different cells without cross-contamination because it can be equipped with a connecting hatch to multiple CO_2 incubators. Large-scale production and multi-sample cell culture capacity for cell transplantation may be a prerequisite for commercialization of cell products under current good manufacturing practice (cGMP) grade. Production methods for cell therapy should be designed to ensure that the end product is standardized and safe. cGMP is a quality assurance system that ensures that the cell product meets preset specifications with minimal lot-to-lot variability [23]. It requires traceability of raw materials used in cell culture and validated standard operating procedures (SOPs) throughout the process [24,25]. Current good tissue practice (cGTP) is intended to prevent human cells, tissues, and cellular and tissue-based products from contamination by infectious disease agents and to ensure that these cells and tissues maintain their integrity and function. The controlled environment of a carefully designed, constructed, validated, and maintained clean room will minimize the risks of environmental contamination and decrease the possibility of cross-contamination [26]. Based on cGMP, aseptic handling and filling of raw materials should be performed in a grade A environment (class 100) with a grade B background (class 1,000). Clean room disciplines, gowning procedures, cleaning programs, and maintenance of air handling units are included in SOPs. Environmental monitoring is essential in clean room quality control. Proper cleaning, maintenance, repair, and attire are major issues for cGMP [27].

Construction and maintenance of a cGMP facility is so expensive that it may be difficult to conform to these standards on a large scale without automation. Unlike manual culture, the robots enabled the environment in the cell culture cabinet to be completely separated from the external environment. Moreover, automated cell culture machines can be equipped with cleaning and monitoring systems to prevent contamination by microorganisms and cross-contamination by other cell types cultured in tandem. These properties may meet the stringent conditions for a human cell processing facility while reducing both construction and maintenance costs.

In Japan, the regulatory path of a regenerative cell therapy using this automated machine will be to obtain an approval for the end products, such as cells or tissues, based on the new guidelines and philosophy at an initial phase. An important requirement for obtaining approval is publication of the safety and reliability of the machine to produce the final biological products in a peer-reviewed journal. The similar properties of cell products between those obtained by machine and those obtained by manual culture, as demonstrated in this study, could support approval of a clinical trial using this machine, which is currently being planned.

Conclusion

AutoCulture® is one of the best candidates to solve the problems inherent in large-scale production and harvesting of human cells for clinical applications. The automated cell processing system can reproduce many complex operations performed by professional staff and can maintain multiple cell lines automatically. Thus, this automation system will be a powerful tool for both clinical trials exploring the potential of autologous or allogeneic cell-based regeneration therapies and for the commercialization.

Methods

Isolation of human CSCs containing atrial appendage

After this study was approved by the ethics committees of Tokyo Metropolitan Geriatric Hospital (ID: #220106), human cardiac tissue samples from RAA were surgically excised from 7 patients (60–75 years old) during cardiac surgery. All patients provided written informed consent. A cell population containing CSCs was acquired according to the current protocol for ALCADIA [28]. In brief, the tissue fragments were cut into 5 × 5-mm pieces and incubated with 0.2% collagenase type II and 0.1% DNase I (Worthington Biochemicals) at 37°C for 30 min. The cells were cultivated in a basic culture medium of Dulbecco's modified Eagle medium (DMEM)/F12 supplemented with 10% fetal bovine serum (FBS) and 40 ng/ml basic fibroblast growth factor (bFGF). The cells were seeded in 60-mm dishes coated with collagen type I. The cultured cells were passaged twice, harvested, and frozen until used in this experiment. P2 cell population was utilized as the starting material for this comparison experiment.

Cell expansion and harvesting

After thawing, the cells derived from the human atrium were seeded at 1×10^5 cells per 100-mm culture dish and cultivated for 5–7 days. The cells were split at 1:10 at 80%–90% confluence. The basic culture medium was replaced every 3 or 4 days. For automated culture, we used the same lot of CSCs. After seeding, the culture dishes were placed in the AutoCulture® chamber and transferred into the internal CO_2 incubator by the robot arm (Figure 1A, Additional file 4). For media replacement, the robot arm retrieved the culture dishes from the incubator and set them on a rotating table. The dish covers were removed by the robot arm, a specified amount of medium was discarded, fresh medium was supplied by a new pipette, the covers were returned,